

# SPATIAL AND TEMPORAL DYNAMIC OF THE TROPHIC STATE IN A LARGE AMAZONIAN HYDROELECTRIC RESERVOIR

Curtarelli, M. P.<sup>1</sup>, Ogashawara, I.<sup>1</sup>, Alcântara, E. H.<sup>2</sup>, Lorenzzetti, J. A.<sup>1</sup>, Stech, J. L.<sup>1</sup>

<sup>1</sup> National Institute for Space Research, Remote Sensing Division, São José dos Campos, Brazil.

<sup>2</sup> São Paulo State University, Department of Cartography, Presidente Prudente, Brazil.

## ABSTRACT

We assessed the spatial and temporal dynamic of the trophic state in a large Amazonian hydroelectric reservoir during the Austral wintertime using images acquired by the Operational Land Imager (OLI) sensor on board the Landsat 8 satellite. We used the Spectral Angle Mapper (SAM) algorithm and reference *in situ* spectra to classify the OLI images according to a trophic state index (TSI). The results showed that the use of OLI images and the SAM algorithm were suitable for the mapping of the TSI in the Amazonian reservoirs. In our particular case, the reservoir presented a high spatial and temporal heterogeneity in the TSI during the studied period. However, further studies are needed to better characterize the dynamics of the trophic state and its driven forces.

**Index Terms**— trophic state index, hydroelectric reservoir, Amazon, remote sensing, spectral angle mapper

## 1. INTRODUCTION

Amazonian hydroelectric reservoirs are recognized as an important source of greenhouse gas to the atmosphere [1]. However, a recent study conducted by [2] showed that eutrophication may cause a reversal in the role played by reservoirs in the carbon cycle by promoting atmospheric carbon sequestration. In this way, to better understand the real role of Amazonian reservoirs on the terrestrial carbon cycle it is necessary to continuously monitor the water quality in these environments. Nevertheless, due to the nature of Amazonian reservoirs (e.g., large areas and difficulty access) the monitoring of water quality using traditional methods (i.e., *in situ* measurements) is not a simple task. Remote sensing techniques can be a useful tool for the water quality monitoring in Amazonian reservoirs. These techniques have several advantages over the conventional monitoring methods: (1) they provide a synoptic view of study area, which allows the user to retrieve information from the entire aquatic system; (2) they can acquire data from remote, inaccessible locations; and (3) they can record data over time, providing a historical dataset [3]. Although remote sensing techniques have been

extensively used to study the water quality of inland water located in different regions of the world [4-5] there are few studies conducted at Amazonian region. In this work we used *in situ* data and remote sensing orbital data to study the spatial and temporal heterogeneity of the trophic state of a large hydroelectric reservoir located at Brazilian Amazon. Our main goal was to understand the spatial-temporal dynamic of trophic state (based on chlorophyll-a (chl-a) concentration) and its main environmental driven forces.

## 2. STUDY AREA

The Tucuruí Hydroelectric Reservoir (THR) is located at Brazilian Amazon, Pará State, between 3.75° S; 49.52° W and 5.00° S; 49.58° W. It is one of the greatest hydroelectric reservoirs in the world, with a flooded area of 2,918 km<sup>2</sup> and a total volume of 50.3 billion m<sup>3</sup>. The reservoir is elongated from north to south and is approximately 150 km in length and 20 km in width. The water level varies by 15 m throughout the year, and its dynamic shows 4 stages: rising (Jan to Mar), high (Mar to July), falling (July to Oct) and low (Oct to Dec).

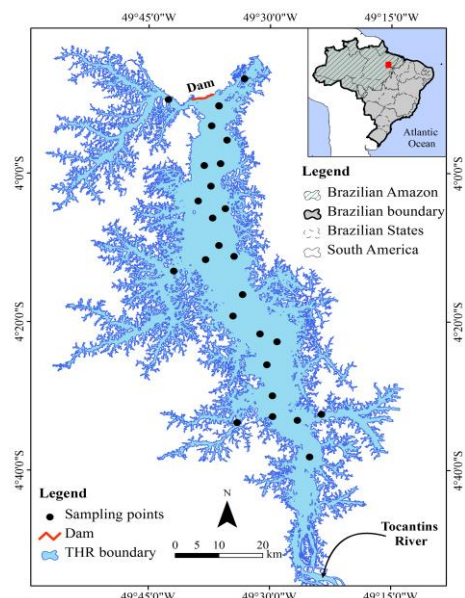


Figure 1. Study area.

### 3. MATERIAL AND METHODS

#### 3.1. In situ dataset

The *in situ* data were collected during one field campaign conducted at THR between 18 and 30 November 2012 (low water level period). The *in situ* dataset includes radiometric measurements and chl-*a* concentrations obtained at 24 sample points distributed throughout the reservoir (see Figure 1 for location). The radiometric measurements were conducted using a FieldSpec HandHeld 2™, ASD (Boulder, CO, USA), following the protocol presented by [6]. To determine the chl-*a* concentrations, water samples were kept cool until they arrived on land where they were filtered through Whatman® GF/F filters and stored frozen (-20°C) until further analysis in the laboratory. Filters were analyzed as described in [5].

#### 3.2. Remote sensing dataset

Three images (path 224, row 63) were acquired between 16 June and 3 August 2013 (high and falling water level periods) by the OLI, a multispectral sensor on board Landsat 8 satellite [7]. The Table 1 summarizes the main characteristics of OLI sensor [8]:

Table 1. Summary of the main characteristics of the OLI product.

Temporal coverage	Since February 11 2013
# of spectral bands	9 bands
Pixel size	30 m and 15m
Radiometric quantization	16 bits
Temporal resolution	16 days
Scene size	170 km (N-S) by 183 km (W-E)
Projection	Universal Transverse Mercator
File size	~1 Gb (compressed)

The OLI images were obtained freely through USGS Global Visualization (GLOVIS) portal <<http://glovis.usgs.gov/>>. The standard Landsat 8 OLI product provided by the GLOVIS consists of quantized and calibrated scaled digital numbers (DN) delivered in 16-bit unsigned integer format. The OLI images are available in an orthorectified grid with 30 m spatial resolution for the multispectral channels (bands 1-7 and 9) and 15 m for the panchromatic channel (band 8). The DN values were converted to the Top of Atmosphere (TOA) radiance using the radiometric rescaling coefficients provided in the product metadata file and the equations provided

at <[http://landsat.usgs.gov/Landsat8\\_Using\\_Product.php](http://landsat.usgs.gov/Landsat8_Using_Product.php)>.

After the conversion to TOA radiance, the images were atmospheric corrected using the Fast Line-of-sight Atmospheric Analysis of Spectral Hypercubes (FLAASH) module of Environment for Visualizing Images (ENVI®) software and converted into surface reflectance. The OLI relative spectral response sampled at 1nm intervals were

obtained at <[http://landsat.gsfc.nasa.gov/wp-content/uploads/2013/06/Ball\\_BA\\_RSR.v1.1-1.xlsx](http://landsat.gsfc.nasa.gov/wp-content/uploads/2013/06/Ball_BA_RSR.v1.1-1.xlsx)>.

#### 3.3. Spectral Angle Mapper algorithm

The SAM algorithm [9] was applied to all OLI atmospheric corrected images to discriminate the different water mass into the reservoir. The classification was conducted based on reference spectra obtained using the *in situ* dataset. Six reference spectra were defined based on the TSI [10]: oligotrophic (1.17 to 3.24 µg L⁻¹), mesotrophic (3.24 to 11.03 µg L⁻¹) eutrophic (11.03 to 30.55 µg L⁻¹), supereutrophic (30.55 to 69.05 µg L⁻¹) and hypereutrophic (> 69.05 µg L⁻¹). Before the classification the reference spectra were resampled to the OLI bands. During the classification different angles from 0.2 to 0.5 were tested in the SAM algorithm.

### 4. RESULTS

The THR showed a high spatial heterogeneity in the TSI, with 6 distinct classes identified with the *in situ* dataset. The Figure 2 shows the 6 reference spectra obtained from *in situ* dataset and used to classify the OLI images using the SAM algorithm.

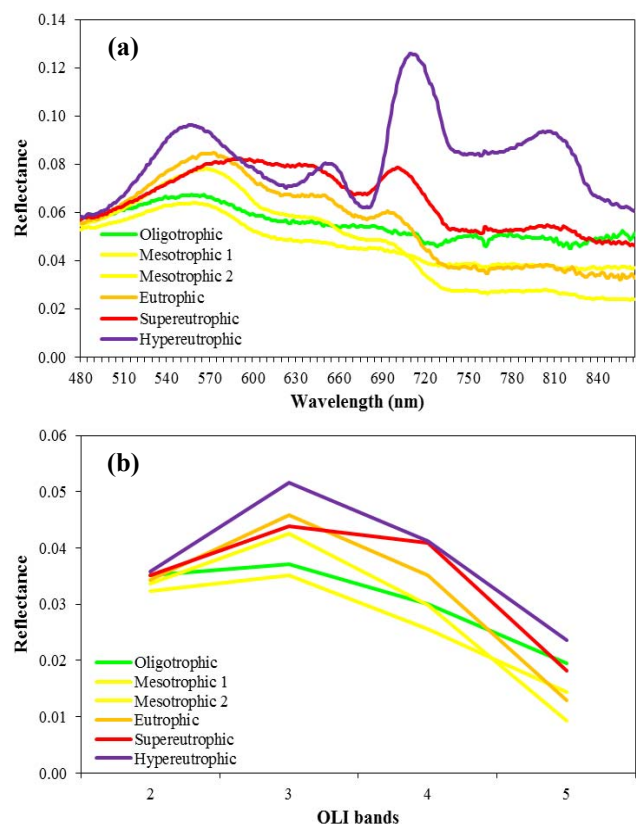


Figure 2. Reference spectra: (a) original data and (b) spectra resampled to OLI bands 2, 3, 4 and 5.

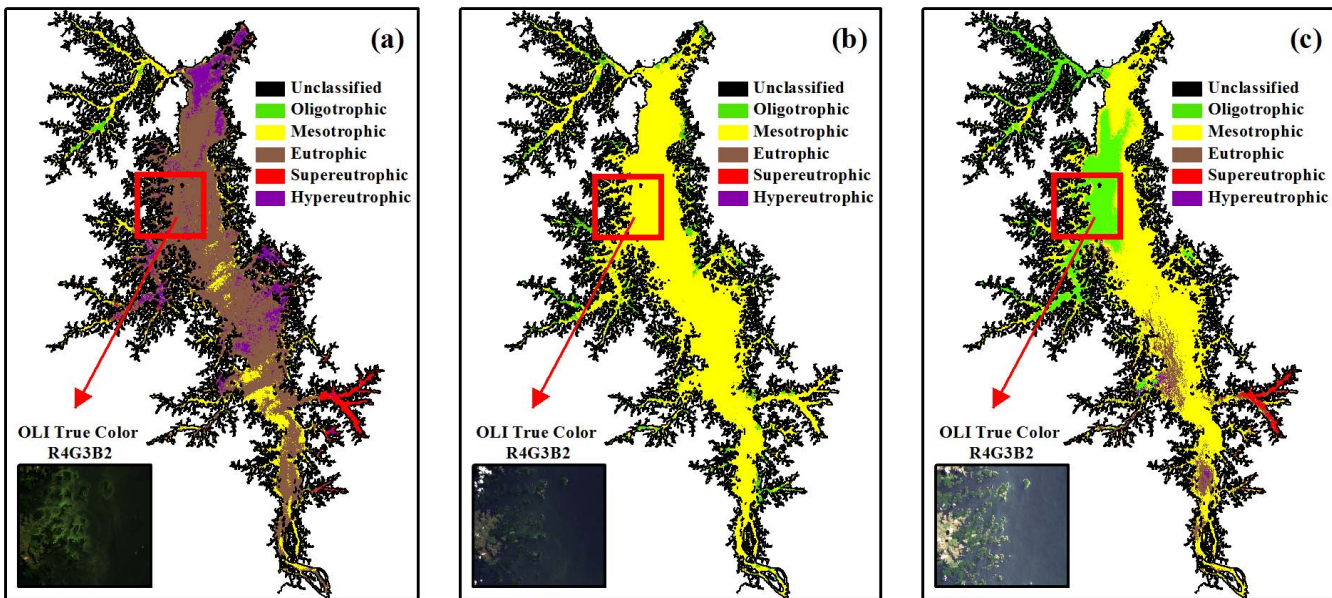


Figure 3. Spatial-temporal variation of trophic state retrieved using the SAM algorithm: (a) 16 June 2013, (b) 18 July 2013 and (c) 3 August 2013.

Among the 24 samples collected only 1 showed chl-*a* concentration lower than  $3.24 \mu\text{g L}^{-1}$  and was classified as oligotrophic ( $2.8 \mu\text{g L}^{-1}$ ). The hypereutrophic ( $798.9 \mu\text{g L}^{-1}$ ), supereutrophic ( $39.5 \mu\text{g L}^{-1}$ ) and eutrophic ( $14.0 \mu\text{g L}^{-1}$ ) classes also have only 1 representative sample for each class. All the others 20 samples were classified as mesotrophic (ranging from  $3.5$  to  $10.8 \mu\text{g L}^{-1}$ ). For the mesotrophic class two characteristic spectra were observed in the dataset. In this case, we used the two spectra as reference for this class (mesotrophic 1 and 2) in the classification algorithm (see Figure 2).

All the angles tested in the SAM algorithm produced visually identical classification results but the number of unclassified pixels was the lowest for the angle of 0.5. Therefore, the results presented in this study are for this angle. Figure 3 shows the spatial and temporal evolution of the TSI during the period analyzed. For the image collected on 16 June 2013 (Fig. 3a) most of the reservoir was classified as eutrophic (47%), with some areas classified as oligotrophic (1%), mesotrophic (22%), supereutrophic (3%) and hypereutrophic (9%); 18% of image was unclassified. In the second image, collected on 18 July 2013 (Fig. 3b), most of reservoir was classified as mesotrophic (71%) with small areas classified as oligotrophic (14%) and 15% of unclassified pixels. On 3 August 2013 (Fig. 3c) most of reservoir was classified again as mesotrophic (51%) with some areas classified as oligotrophic (20%), eutrophic (6%), supereutrophic (2%) and hypereutrophic (3%); 18% of pixels were unclassified. In the three dates analyzed the high TSI (chl-*a* concentrations) was observed at the transition and littoral zones. The spatial and temporal variability of the TSI was consistent with visual inspection of images (true color

composition, R4G3B2) and previous three-dimensional modeling study which simulated different water quality parameters in the THR [11]. The spatial and temporal heterogeneity of trophic state observed in the THR can be related with the reservoir hydrodynamic and the nutrients intake, which in turn are influenced by the hydrologic cycle.

## 5. FINAL CONSIDERATIONS

In this study we investigated the spatial and temporal dynamics of the TSI (based on chl-*a* concentration) in a large Amazonian hydroelectric reservoir using Landsat 8 OLI images and the SAM algorithm. The main conclusions are:

From the spatial and temporal point of view, the THR showed a quite variable TSI during Austral wintertime (high and falling water level stages). Along this season the higher TSI values (eutrophic, supereutrophic and hypereutrophic stages) were observed at transition and littoral zone where the nutrients supply is generally higher than in the main body of the reservoir.

The OLI spectral bands and the SAM algorithm showed to be suitable for the mapping of TSI in Amazonian reservoirs. The spectral resolution of OLI images allows detecting different water masses with distinct spectral response and a wide range of chl-*a* concentration.

Preliminary results obtained using a hydrodynamic model (not shown in this study) indicates that the vertical mixing and the water circulation are the two main physical factors controlling the dynamics of the TSI at THR.

Further studies are needed to better characterize the dynamics of the trophic state in the THR and its driven forces. Also, the impact of short time-scale meteorological

events (e.g., mesoscale convective systems) on the spatial and temporal variability of the TSI needs to be investigated. As suggestions for future studies we recommended the integration of remote sensing-derived information and three-dimensional hydrodynamic models to investigate the physical processes governing the TSI variability in the THR.

## 6. ACKNOWLEDGEMENTS

The authors wish to thanks Joaquim Antônio Dionísio Leão, Carlos Alberto Sampaio Araujo and Dr. Claudio Clemente Faria Barbosa for their assistance during the field campaign. The field campaign was supported by Northern Brazil Electric Power Company (ELETRONORTE, grants 4500075234), Brazilian Electricity Regulatory Agency (ANEEL, grants 8000003629) and the Graduate Program in Remote Sensing sciences of the National Institute for Space Research (PGSER/INPE). The authors also thanks the National Institute of Science and Technology for Climate Change (grant 573797/2008-0 CNPq) for the financial support and the Hidrosfera Research Group at the Remote Sensing Division (DSR) of INPE for the technical support. The first author is grateful to the Brazilian Council of Technological and Scientific Development (CNPq) for the doctorate scholarship (under grants 161233/2013-9).

## 7. REFERENCES

- [1] N. Barros, J.J. Cole, L.J. Tranvik, Y.T. Prairie, D. Bastviken, V.L.M. Huszar, P. del Giorgio and F. Roland, "Carbon emission from hydroelectric reservoirs linked to reservoir age and latitude," *Nature Geoscience*, Nature Publishing Group, London, pp. 593-596, 2011.
- [2] F.S. Pacheco, F. Roland and J.A. Downing, "Eutrophication reverses whole-lake carbon budgets," *Inland Waters*, Freshwater Biological Association, Ambleside, pp. 41-48, 2014.
- [3] D.G. Hadjimitsis and C. Clayton, "Assessment of temporal variations of water quality in inland water bodies using atmospheric corrected satellite remotely sensed image data," *Environmental Monitoring and Assessment*, Springer, São Paulo, pp. 281-292, 2009.
- [4] T. Kutser, B. Paavel, C. Verpoorter, T. Kauer and E. Vahtmäe, "Remote sensing of water quality in optically complex lakes," *International Archives of the Photogrammetry*, International Society for Photogrammetry and Remote Sensing, Melbourne, pp. 165-169, 2012.
- [5] I. Ogashawara, D.R. Mishra, S. Mishra, M.P. Curtarelli and J.L. Stech., "A performance review of reflectance based algorithms for predicting phycocyanin concentrations in inland waters," *Remote Sensing*, MDPI, Basel, pp. 4774-4798, 2013.
- [6] J.L. Mueller, A. Morel, R. Frouin, C. Davis, R. Arnone, K. Carder, Z.P. Lee, R.G. Steward, S. Hooker, C.D. Mobley, S. McLean, B. Holben, M. Miller, C. Pietras, K.D. Knobelspiesse, G.S. Fargion, J. Porter and K. Voss, "Above-water radiance and remote sensing reflectance measurements and analysis protocols. Ocean Optics protocols for satellite ocean color sensor validation Revision 2," National Aeronautics and Space Administration, Greenbelt, pp. 98-107, 2000.
- [7] J.R. Irons, J.L. Dwyer and J.A. Barsi, "The next Landsat satellite: The Landsat Data Continuity Mission," *Remote Sensing of Environment*, Elsevier, New York, pp. 11-21, 2012.
- [8] United States Geological Survey (USGS), "Landsat 8," Available at <http://landsat.usgs.gov/landsat8.php>. Accessed on 13 May 2014.
- [9] F.A. Kruse, A.B. Lefkoff, J.W. Boardman, K.B. Heidebrecht, A.T. Shapiro, P.J. Barloon and A.F.H. Goetz, "The Spectral Image Processing System (SIPS) - Interactive visualization and analysis of imaging spectrometer data," *Remote Sensing of Environment*, Elsevier, New York, pp. 145-163, 1993.
- [10] M.C. Lamparelli, "Grau de trofia em corpos d' água do Estado de São Paulo: avaliação dos métodos de monitoramento," *PhD Thesis* (in portuguese), Universidade de São Paulo, São Paulo, pp. 1-135, 2004.
- [11] R. Deus, D. Brito, I.A. Kenov, M. Lima, V. Costa, A. Medeiros, R. Neves and C.N. Alves, "Three-dimensional model for analysis of spatial and temporal patterns of phytoplankton in Tucuruí reservoir, Pará, Brazil," *Ecological Modelling*, Elsevier, New York, pp. 28-43, 2013.